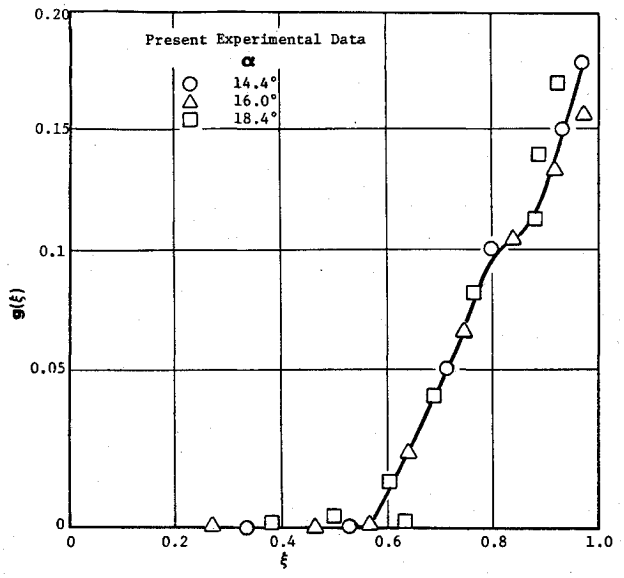

Fig. 4 Similarity parameter for the back-flow region of the separated velocity profile.

useful in developing calculation methods for separated boundary layers.

The reversed flow is influenced by a number of factors. First, the back flow could be considered a wall flow with scales based on wall shear stress. Simpson et al.[11] showed that these scales could not correlate their data. They also demonstrated that downstream flowfield conditions influence the magnitude of the back flow in a nonattaching separated boundary layer. Therefore, it seems that the back flow is a complex regime in which wall and outer flow variables in addition to downstream conditions may be important. Hence, it appears that the flow scales form on local variables. Simpson et al.[11] proposed the maximum back-flow velocity and its distance from the wall as two scales. These gave a fair correlation of their data.

In the present analysis, u_n was used as the velocity scale. However, y_2 as defined in Eq. (4) was selected as the length scale in contrast to studies by Simpson et al.[11] As seen in Figs. 2a and 3a, the maxima in the back-flow profiles tend to be rather flat ($du/dy \sim 0$). As a result, it was decided to curve-fit this data numerically and select y_2 as a distance where du/dy became positive. This length scale was selected for the following reasons. First, it provided the required matching point between the outer, mixing region flow and the back flow. Second, the length scale selected by Simpson et al.[11] would be more representative of the wall region only, and would incorporate the influence of the outer flow to a lesser degree. In contrast, y_2 incorporates the influence of the outer flow. As a result, it would seem to be an appropriate choice for the length scale in the back-flow region.

Figure 4 depicts the back-flow velocity plotted in the similarity coordinates:

$$\xi = (y_2 - y)/y_2 \tag{4}$$

$$g(\xi) = (u_n - u)/u_n \tag{5}$$

As can be seen, even with a limited amount of data in this region a good correlation is obtained.

It must be pointed out that for the airfoil flow (increasingly adverse pressure gradient) both u_n and y_2 increase in the streamwise direction. In contrast, the law-of-the-wall length scale ν/u_τ varies inversely with its velocity scale u_τ.

Concluding Remarks

Separated flow measurements on the upper surface of the NASA GA(W)-1 airfoil show that it is possible to divide the separated velocity profile into three viscous regions: the wall boundary layer, the transition region, and the external half wake. In the back-flow region, the mean velocity is found to demonstrate self-similarity behavior that is distinct from the law-of-the-wall for the turbulent boundary layers. In addition, the mixing region profiles show self-preserving behavior such that the chordwise development of the mean velocity is found to be reducible to a universal curve.

Acknowledgment

Parts of this work were performed under the NASA Contract NAS1-13985.

References

[1]Kline, S. J., "Some New Conceptions of the Mechanism of Stall in the Turbulent Boundary Layers," *Journal of the Aeronautical Sciences,* Vol. 24, 1957, pp. 470–471.

[2]Simpson, R. L., Strickland, J. H., and Barr, P. W., "Features of a Separating Turbulent Boundary Layer in the Vicinity of Separation," *Journal of Fluid Mechanics,* Vol. 79, 1977, pp. 553–594.

[3]Samuel, A. E. and Joubert, P. N., "A Boundary Layer Developing in an Increasingly Adverse Pressure Gradient," *Journal of Fluid Mechanics,* Vol. 66, 1974, pp. 481–505.

[4]Chu, J. and Young, A. D., "Characteristics of a Separated Incompressible Turbulent Boundary Layer," AGARD CP-168, No. 13, 1976.

[5]Clauser, F. H., "Turbulent Boundary Layers in Adverse Pressure Gradients," *Journal of Aerospace Sciences,* Vol. 21, 1954, pp. 91–108.

[6]Perry, A. E. and Schofield, W. H., "Mean Velocity and Shear Stress Distributions in Turbulent Boundary Layers," *Physics of Fluids,* Vol. 16, 1973, pp. 2068–2074.

[7]Schofield, W. H., "On Separating Turbulent Boundary Layers," Department of Defense Rept. 162, Aeronautical Research Laboratories, Australia.

[8]Whitcomb, R. T. and Heath, A. R., "Several Methods for Reducing the Drag of Transport Configurations at High Subsonic Speeds," NASA Memo 2-25-591, 1975.

[9]Goradia, S. H., Mehta, J. M., Shrewsburry, G. S., "Analyses of the Separated Boundary Layer on the Surface and in the Wake of Blunt Trailing Edge Airfoils," NASA CR-145202, April 1977.

[10]Mehta, J. M. and Goradia, S. H., "Experimental Studies of the Separated Flow Over a NASA GA(W)-1 Airfoil," *AIAA Journal,* Vol. 22, 1984, pp. 552–554.

[11]Simpson, R. L., Chew, Y. T. and Shivaprasad, B. G., "The Structures of a Separating Turbulent Boundary Layer. Part 1. Mean Flow and Shear Stresses," *Journal of Fluid Mechanics,* Vol. 113, 1981, pp. 23–51.

Self-Preservation of Turbulent Wakes

Jayesh M. Mehta*
Illinois Institute of Technology, Chicago, Illinois

Nomenclature

b	= half wake-width
c	= chord of the airfoil
$h(\zeta)$	= wake similarity parameter
M	= freestream Mach number
Re	= freestream Reynolds number
u	= mean velocity
w	= wake velocity defect

Received April 20, 1987; revision received Oct. 21, 1987.

*Graduate Student, Department of Mechanical Engineering; currently with Combustion and Heat Transfer Technology, Aircraft Engine Business Group, General Electric Co., Everdale, OH. Member AIAA.

w_0 = maximum wake velocity defect
W_0 = wake similarity parameter, Eq. (2)
W_0^* = asymptotic value of W_0
x_b = downstream distance from the trailing edge in the wake
y_w = vertical distance in the wake
α = angle of attack
Δ = wake similarity parameter, Eq. (1)
θ_w = wake deficit momentum thickness, Eq. (3)
ν_t = eddy viscosity
ρ = density
ζ = similarity parameter, Eq. (5)

Introduction

STRUCTURE of far wakes is well described by classical theories. There also exist excellent sets of experimental data on two-dimensional asymptotic far wakes.[1,2] However, these do not provide any information on evolution of the near wake into an asymptotic state. These evolution processes are known to be quite different for different wake generators, including nonseparating bodies, such as flat plates and airfoils. Recently, Sreenivasan[3] has examined the manner in which plane turbulent wakes, behind wake generators of different shapes, approach a self-preserving (asymptotic) state. In the study, several different types of wake generators, such as circular and square cylinders, flat plates, and twin plates, were studied at Reynolds numbers (based on momentum thickness) ranging from 1020 to 4500.

The purpose of this Note is to examine the manner in which the turbulent wakes behind sharp and blunt trailing edge NASA GA(W)-1 airfoils[4] approach a unique self-preserving state. First, a new set of data is presented for the separated near wake. Second, the flow development in the near wake is analyzed, and its development processes are compared with those behind several other wake generators (e.g., a circular cylinder). Finally, mean velocity profiles measured in the far wake are evaluated for flowfield similarity.

Experiments

All the experiments were performed in the wakes of sharp and blunt trailing edge airfoils. Figure 1 shows schematic of the airfoil section. As can be seen, blunt trailing edge airfoil was fabricated by removing the last 7% of the chord length from the corresponding sharp trailing edge airfoil. The resulting blunt trailing edge airfoil section had a chord length of 0.26 m and a span of 0.76 m.

Total pressure data in the wake were acquired by a special dual-purpose pressure sensor, consisting of two probes. One probe pointed downstream, and the other faced upstream. Both probes were fabricated of 0.0013 m tubing, that was flattened to 0.00065 m at the end. A semicircular disc type pressure probe (0.0032 m diam and 0.0016 m thickness) was used for static pressure measurements.

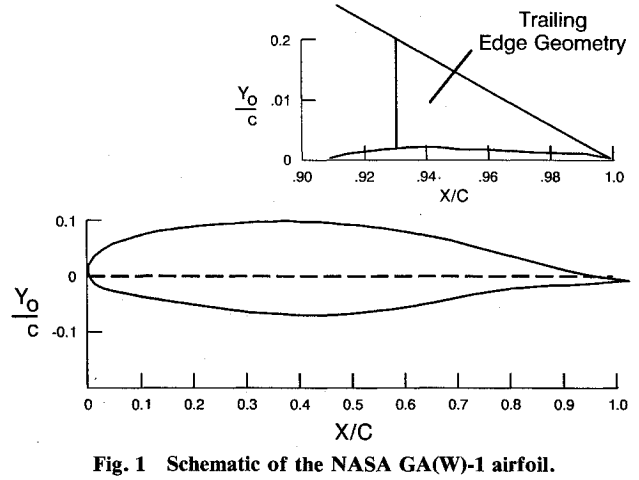

Fig. 1 Schematic of the NASA GA(W)-1 airfoil.

Two major sources of errors exist when measurements are made in the wake using these probes. They arise due to high sensitivity of the disc probes to turbulence intensity and unsteadiness of the flow. However, results from the total-static probe combination were found to be generally repeatable within $\pm 4\%$, even under separated wake flow conditions. Hence, they are presented here without any corrections for these effects. A detailed description of measuring sensors as well as data acquisition and processing systems is given in Ref. 5.

Streamwise development of mean velocity profiles in the wake of the blunt trailing edge airfoil is depicted in Fig. 2. These data were acquired at $\alpha = 14.4$ deg, $M = 0.18$, and $Re = 2 \times 10^6$. In Fig. 2, the boundary layer is thicker, and separated on the upper trailing edge ($x_b/c = 0$), compared to that on the lower trailing edge. This can be attributed to strong adverse pressure gradient that exists on the upper surface. It also influences the wake development in the immediate vicinity of the trailing edge. As seen in the figure, for about 10% of the chord length, changes in the upper part and in the inner region of the wake are more pronounced than in the lower part. The velocity profiles are clearly asymmetric and, for a larger part, the lower wake shows no development. For distances greater than 10% of the chord length, classical fuller wake profiles are observed. However, they are still asymmetric and remain asymmetric, even at the last measurement station ($x_b/c \sim 0.91$).

Narsimha and Prabhu[6] have demonstrated that in the asymptotic limit of a vanishing defect, a self-preserving turbulent wake is characterized by constant values of the following two parameters. These are defined as

$$\Delta = b^2/(x_b \cdot \theta_w) \tag{1}$$

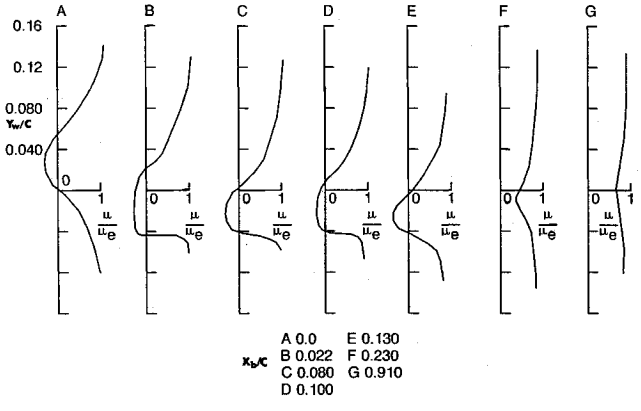

Fig. 2 Measured mean velocity profiles in the wake of the blunt trailing edge airfoil.

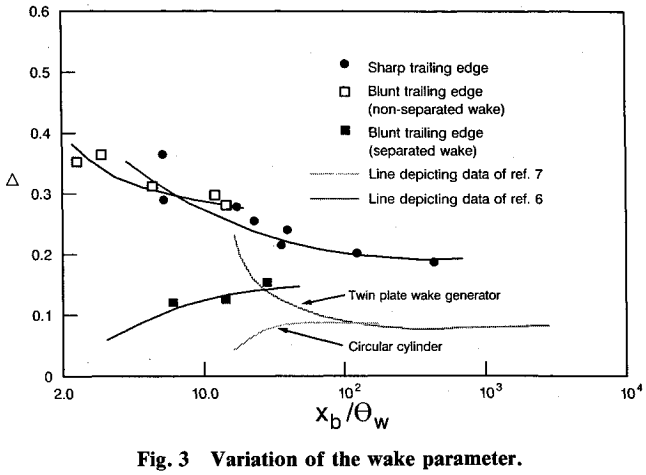

Fig. 3 Variation of the wake parameter.

and

$$W_0 = (w_0/u_e)(x_b/\theta_w)^{1/2} \tag{2}$$

In Eqs. (1) and (2), the wake deficit momentum thickness θ_w is defined as

$$\theta_W = \int_{-\infty}^{\infty} (w/w_0)\,[1-(w/w_0)]\,dy \tag{3}$$

Figure 3 depicts the variation of parameter Δ as a function of x_b/θ_w for wakes generated by blunt and sharp trailing edge airfoils. Separated and nonseparated flows in the near wake of the blunt trailing edge airfoil have been analyzed. The figure also depicts the results of Narsimha and Prabhu,[6] and Townsend[7] for comparison. Both Townsend's results[7] and the results of Ref. 6, correspond to the wake behind a circular cylinder.

As premised in Ref. 6, Δ is one of two parameters characterizing processes by which wake profiles achieve an asymptotic state. In Fig. 3, the wakes behind a cylinder and a twin-plate wake generator reach the asymptotic state via two different routes. However, they both reach an asymptotic value of 0.10 downstream of $x_b/\theta_w = 100$. For the airfoil-type wake generators, the wake development occurs in a similar qualitative fashion. First, the separated wake follows the path of the wake behind a circular cylinder closely, while the nonseparated wakes behind the sharp and blunt trailing edge airfoils follow the path of the wake behind a twin-plate wake generator. Second, in each of the previous cases, the parameter reaches an asymptotic value, such that for the separated wake, Δ^* has an asymptotic value of 0.16, while for the nonseparated wake (behind the blunt trailing edge airfoil), it is 0.28. The nonseparated wake behind the sharp trailing edge airfoil follows the path of the twin-plate wake generator most closely. However, the asymptotic value of parameter Δ^* for this case is higher than that of the twin-plate generator. For the sharp trailing edge airfoil, it is 0.20.

Next, the variation of parameter W_0 with w_0/u_e, is depicted in Fig. 4. The figure also shows results of Refs. 6 and 7 for comparison. As can be seen, different wakes reach self-preservation through different routes. Evidently, the wake behind the twin-plate wake generator,[6] has the simplest behavior as it reaches the asymptotic state in the shortest duration. The nonseparated wakes behind the sharp and blunt trailing edge airfoils depict extreme degrees of variability and nonmonotonic behavior, before both reach the asymptotic state. The asymptotic value of parameter W_0 (at $w_0/u_e \to 0$), were determined to be 1.10.

Separated wake behind the blunt trailing edge airfoil depicts the most aberrant nature by which it achieves self-preserved state. In particular, its behavior in the region where the defect reaches a small (but finite) value is difficult to evaluate. From limited available data, the asymptotic value for parameter W_0^*, is estimated to be much lower than the corresponding value for the nonseparated wake.

One of the interesting issues that arise in the discussion of wake development, is being concerned with downstream distance from the trailing edge beyond which the wake is regarded as having reached an asymptotic state. Associated with this issue is labeling of the wake as near wake and far wake. In the far wake, the assumption of small velocity defect leads to well-known half power laws for half-width b, and the maximum velocity defect w_0. If it is further assumed that the eddy viscosity ν_t is constant across the wake,[8] then the shear stress τ and velocity defect w are given by

$$\tau/\rho w_0^2 = 8(\ell n 2)(\nu_t/w_0 b)\,\exp(-4\zeta^2 \ell n 2)$$

$$w/w_0 = \exp(-4\zeta^2 \ell n 2) \tag{4}$$

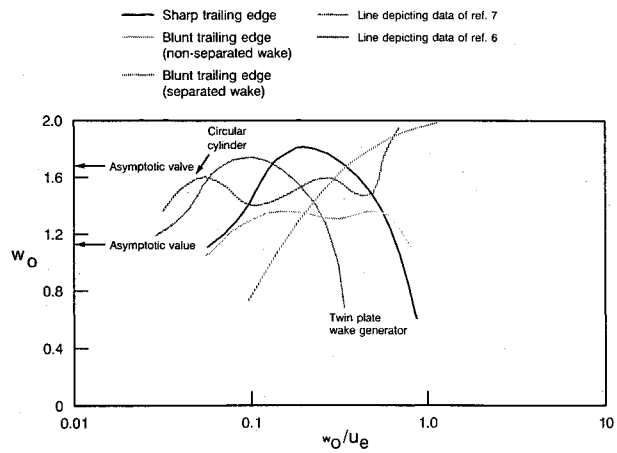

Fig. 4 Variation of the wake parameter.

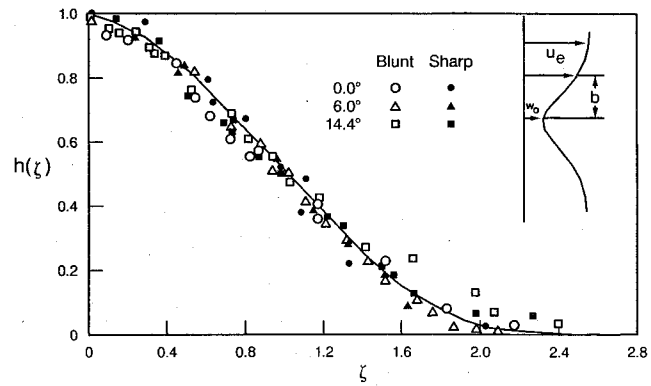

Fig. 5 Mean velocity profiles in the wake similarity coordinates.

where

$$\zeta = y_w/b \tag{5}$$

The above ideas for flowfield similarity are tested here for the far wake of GA(W)-1 airfoils. Figure 5 shows velocity-defect profiles in the far-wake coordinates, ζ and $h(\zeta)$. Here, $h(\zeta)$ is w/w_0. Data presented in this figure also include the defect profiles obtained in the wake of the sharp trailing edge GA(W)-1 airfoil. It is seen that the measured profiles for the blunt and sharp trailing edge airfoils agree well with each other. When viewed collectively with the results of Figs. 3 and 4, it leads to the following observation. The nature of the boundary layer upstream of the trailing edge may not have a significant influence on self-preserving characteristics of the mean velocity profile. However, it influences the processes by which self-preservation is achieved. There are substantial differences in them, especially when the defect ratio (w_0/u_e) is low.

Concluding Remarks

An experiment has been presented that describes wake flow development behind NASA GA(W)-1 airfoils. The measurements show that in the far wake, the mean velocity profiles demonstrate self-similar behavior irrespective of the nature of the upstream boundary layer. However, the processes by which different wakes reach the asymptotic state are much different for different types of wake generators.

Acknowledgment

Parts of this work were performed under the NASA Contract NAS1-13985.

References

[1]Townsend, A. A., "Self-Preserving Flow Inside a Turbulent Boundary Layer," *Journal of Fluid Mechanics,* Vol. 22, April 1965, pp. 773-797.

[2]Prabhu, A. A., "Non-Equilibrium Wakes," Ph.D. Dissertation, Indian Institute of Science, Bangalore, India, 1971.

[3]Sreenivasan, K. R., "Approach to Self-Preservation in Plane Turbulent Wakes," *AIAA Journal,* Vol. 19, Oct. 1981, pp. 1365-1367.

[4]Whitcomb, R. T. and Heath, A. R., "Several Methods for Reducing the Drag of Transport Configurations at High Subsonic Speeds," NASA Memo 2-25-591, 1975.

[5]Goradia, S. H., Mehta, J. M., and Shrewsburry, G. S., "Analyses of the Separated Boundary Layer on the Surface and in the Wake of Blunt Trailing Edge Airfoils," NASA CR-145202, April 1977.

[6]Narsimha, R. and Prabhu, A., "Equilibrium and Relaxation in Turbulent Wakes," *Journal of Fluid Mechanics,* Vol. 54, July 1972, pp. 1-17.

[7]Townsend, A. A., *The Structure of Turbulent Shear Flow,* Cambridge Press, 1956.

[8]Schlichting, H., *Boundary Layer Theory,* 6th ed., McGraw-Hill, New York, 1968.

Errata

Boundary-Layer Transition Effects on Airplane Stability and Control

C. P. van Dam
University of California, Davis, Davis, California
and
B. J. Holmes
NASA Langley Research Center, Hampton, Virginia

[JA 25, pp. 702-709 (1988)]

FIGURES 7-9 of this paper were mistakenly switched during production. They appear here in their correct order and with correct captions.

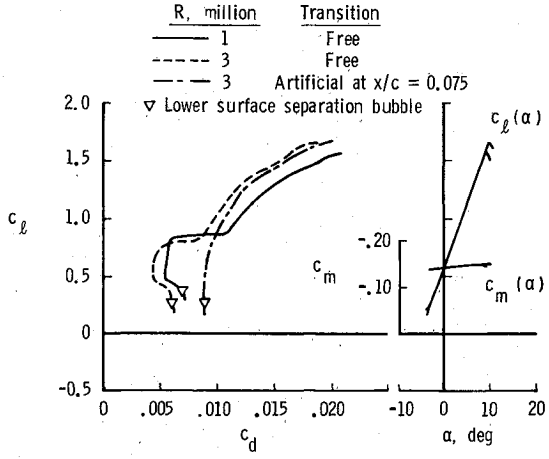

Fig. 7 Calculated aerodynamic characteristics of winglet airfoil section.

The AIAA Editorial Staff regrets any inconvenience this error may have caused our readers.

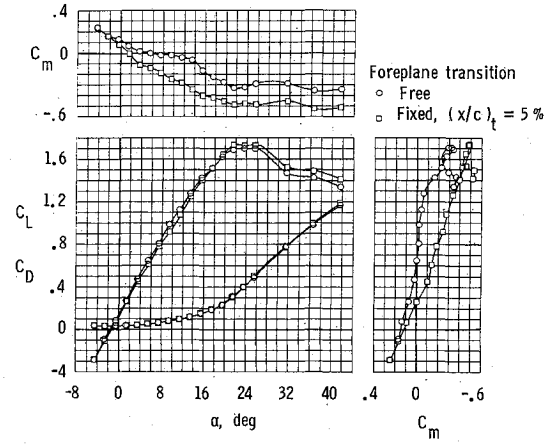

Fig. 8 Longitudinal aerodynamic characteristics of a canard configuration as tested in NASA Langley 30 × 60 ft wind tunnel.

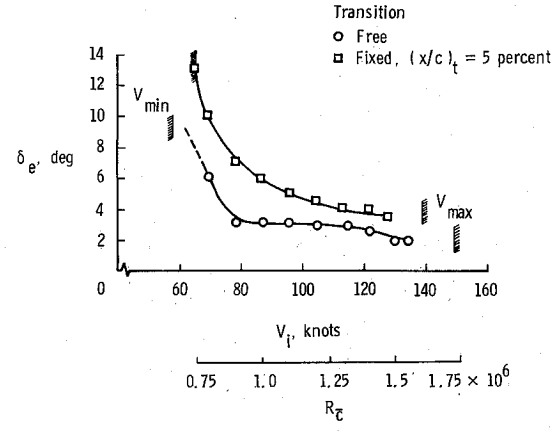

Fig. 9 Flight measured longitudinal control characteristics for VariEze canard-configured airplane ($\bar{c}$ = 1.08 ft).